

Improved laser-EXAFS studies of aluminium foil

To cite this article: R W Eason *et al* 1984 *J. Phys. C: Solid State Phys.* **17** 5067

View the [article online](#) for updates and enhancements.

You may also like

- [Bond compressibility and bond Grüneisen parameters of CdTe](#)
P Fornasini, R Grisenti, T Irifune *et al.*
- [Large negative thermal expansion of the Co subnetwork measured by EXAFS in highly disordered Nd_{1-x}Co_x thin films with perpendicular magnetic anisotropy](#)
J Díaz, R Cid, A Hierro *et al.*
- [Low-dimensional systems investigated by x-ray absorption spectroscopy: a selection of 2D, 1D and 0D cases](#)
Lorenzo Mino, Giovanni Agostini, Elisa Borfecchia *et al.*

Improved laser-EXAFS studies of aluminium foil

R W Eason^{†||}, D K Bradley[‡], J D Kilkenny[‡] and G N Greaves[§]

[†] Laser Division, Rutherford Appleton Laboratory, Chilton, Didcot, Oxon, UK

[‡] Department of Physics, Imperial College, Prince Consort Road, London SW7 2BZ, UK

[§] Daresbury Laboratory, Daresbury, Warrington WA4 4AD, UK

Received 6 March 1984

Abstract. Using a laser-produced plasma as the x-ray source, and a dispersive spectrometer, EXAFS measurements of Al foil have been made that compare favourably with data obtained using a scanning monochromator and soft x-ray synchrotron radiation. Fourier transform analysis yields a radial distribution function for metallic Al that is realistic out to 6 or 7 Å. Compared with other laser-produced plasma EXAFS studies the present measurements offer a considerable improvement which is attributed to the use of a heavy-metal target.

1. Introduction

In the EXAFS (extended x-ray absorption fine-structure) technique, the fine structure that is present on the high-energy side of an x-ray absorption edge is used to yield detailed information on the local environment surrounding a particular atom. Using the theoretical expressions for EXAFS (Lee and Pendry 1975) bond lengths, coordination numbers, and often the chemical identities of the surrounding atoms can be deduced. Unlike x-ray diffraction, EXAFS does not rely on long-range order in the material. It is also element specific, as a spectrum can be obtained that relates to a particular atom type in a structure, and thus is a valuable tool for examining multicomponent systems.

The first use of synchrotron radiation (Kincaid and Eisenberger 1975) as an x-ray source for EXAFS experiments has been followed by a huge expansion of interest in this technique. EXAFS facilities are now a standard provision at most synchrotron radiation facilities. More recently it has been demonstrated that EXAFS data collection times, which are typically tens of minutes, can be reduced to less than a second by replacing the scanning two-crystal monochromator customarily used by a fixed dispersing single-crystal spectrometer (Matsushita and Phizackerley 1981, Flank *et al* 1982). This essentially removes the dead-time associated with the scanning mode and enables one to collect the whole spectrum at once. For EXAFS in the soft x-ray region far more dramatic reductions in data collection times have been achieved by using a single pulse of x-rays generated by a laser-produced plasma (LPP) source (Mallozzi *et al* 1979, 1981). LPP sources have the advantage that not only can a complete spectrum be recorded in ≈ 1 ns, thereby reducing the risk of sample damage in the case of materials that are susceptible

^{||} Now at Department of Physics, University of Essex, Wivenhoe Park, Colchester, Essex CO4 3SQ, UK.

to decomposition or radiation damage, but also they offer the unique possibility of performing single-shot time-resolved measurements of transient structures, which can be induced by the x-rays themselves, or some other synchronised external stimulus (Epstein *et al* 1983).

The 'laser-EXAFS' technique reported by Mallozzi *et al* (1979, 1981) has been pursued in our laboratory in an attempt to see just how far this technique can be pushed to provide accurate, quantitative data. To this end, we have repeated some of the measurements by Mallozzi *et al* (1979, 1981) for aluminium and analysed the data using the EXAFS programs available at the SERC Daresbury Laboratory (Pantos and Firth 1983). The results reported here are spectra taken at room temperature of thin aluminium foils, together with the Fourier transform radial distribution functions. In contrast to the published laser-EXAFS data for aluminium (Mallozzi *et al* 1979, 1981) we used a Bi target which yields a Bremsstrahlung spectrum free from any line structure in the region of interest. Although structure in the spectrum of the source can in principle be normalised out, this can be extremely difficult in practice. Also in this laser-EXAFS work the analysis has been performed using phase shift factors (Lee and Pendry 1975, Lee *et al* 1981). This is in line with most other EXAFS studies and allows shells of atoms to be placed at realistic distances with respect of the exciting atom.

2. Experimental procedure

The experiments to record time-integrated EXAFS spectra were performed in the target chamber of the single-beam area of the Central Laser Facility (Eason and Toner 1983). Pulses of approximately 100–150 J, 1 ns duration, at 1.05 μm were generated by the VULCAN laser system (Ross *et al* 1981) then frequency-doubled to provide 30–50 J of 0.53 μm light. Second-harmonic light was used rather than the fundamental 1.05 μm , for two reasons. Firstly the coupling into thermal bremsstrahlung is more efficient for 0.53 μm light as compared with 1.05 μm , resulting in a higher conversion efficiency into x-rays in the wavelength region of interest here (Turner and Mead 1982). The second reason was that trial experiments at 1.05 μm yielded heavily fogged, poor quality spectra, due to fluorescence from hard x-rays and fast-electron production.

The 30–50 J pulses were focused down to ≈ 100 –200 μm spot sizes using an $f1.5$ quartz aspheric doublet lens. Irradiances therefore were in the region of 10^{14} to $6 \times 10^{14} \text{ W cm}^{-2}$. The arrangement used to record the spectra is shown in figure 1. The dispersing crystal, EXAFS sample and x-ray film were all housed in a minispectrometer. Several crystals were used to look at the aluminium K edge, the most suitable being ADP. The x-ray film used was Kodak SB5. This was used in preference to other films such as Kodak NS-2T as firstly the grain size is smaller for SB5 (0.5–1 μm) than for NS-2T (1–2 μm) and secondly it is less prone to fogging by hard x-rays. The physical size of the minispectrometer ($\approx 50 \times 50 \times 10 \text{ mm}^3$) allowed the device to be positioned very close to the plasma, thus utilising the inherent source brightness to good advantage. The EXAFS sample was placed directly over the x-ray film. Both the sample and the film were made sufficiently remote to avoid any source heating effects. As subsequent time-integrated (Eason *et al* 1984) and time-resolved (Bradley *et al* 1984) experiments have shown, positioning of a 2 μm aluminium foil in close proximity (a few millimetres) to the plasma results in a rapid heating of the foil during the laser pulse, due to the absorption of the incident x-rays. The double-slit arrangement on the front of the minispectrometer allowed several possibilities of recording multiple spectra from a single laser shot.

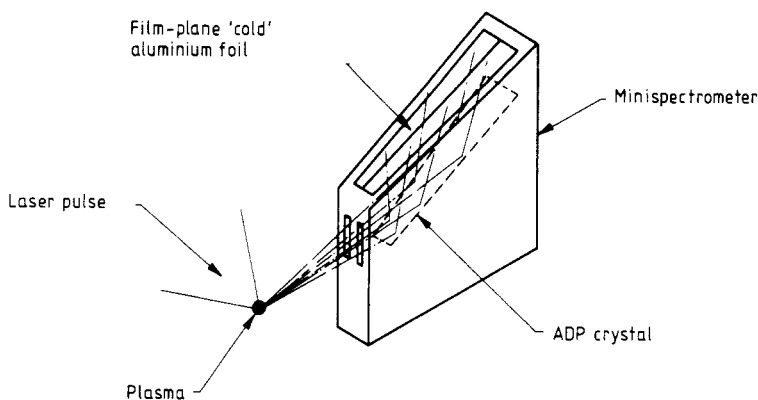


Figure 1. Minispectrometer arrangement used to record laser EXAFS spectrum.

Initially both the incident and transmitted spectra were recorded, by putting a $2\text{ }\mu\text{m}$ aluminium foil over only one half of the film. This allowed the incident x-ray spectrum to be checked for any undesirable line emission in the region of interest. In subsequent experiments, however, double-foil shots were recorded involving two aluminium foils, one over the film plane to provide a 'cold' spectrum and a second at varying distances $\geq 1\text{ mm}$ from the plasma, to provide a 'hot' spectrum. These results are the subject of separate publications (Eason *et al* 1984, Bradley *et al* 1984). For aluminium EXAFS spectra the most suitable target material was found to be bismuth. The target spectrum was examined and found to be structureless to at least 500 eV above the aluminium K edge. Although the incident intensity was approximately the same as in previous work the choice of target material was different from that reported by Mallozzi *et al* (1979, 1981) in which iron was used. The difference between bismuth and iron targets can be clearly seen in figure 2 which shows the microdensitometer traces of two consecutive shots. The first spectrum (shot A) was taken using iron as the target material, whereas for the second (shot B), bismuth was used. In both cases, the front of the minispectrometer was shielded with $25\text{ }\mu\text{m}$ of Be foil, to protect it against visible light. The laser spot size was identical in the two cases and was $\approx 200\text{ }\mu\text{m}$. It is clear that whereas iron shows extensive line emission, bismuth is free from spectral features in this region. The structure present in the iron spectrum has been assigned to Fe XXIV emission lines, according to the tabulations by Boiko *et al* (1978). These lines do serve incidentally as a wavelength calibration for the EXAFS data using bismuth targets, as the minispectrometer position was identical on the two consecutive shots in figure 2. For reference purposes the unattenuated bismuth spectrum is also shown. The observed structure is due to film noise and probably represents a practical limit for signal/noise in this type of experiment. The calculation by Mallozzi *et al* (1981) does not appear to take account of film characteristics so their value for the interval-to-interval contrast ratio is probably over-optimistic.

It is instructive to compare the laser-EXAFS spectrum with a spectrum taken using synchrotron radiation and a scanning monochromator. Fontaine *et al* (1979) have recorded the EXAFS of aluminium foil using the ACO storage ring at LURE. The normalised EXAFS observed by Fontaine *et al* (1979) is reproduced in figure 3, together with

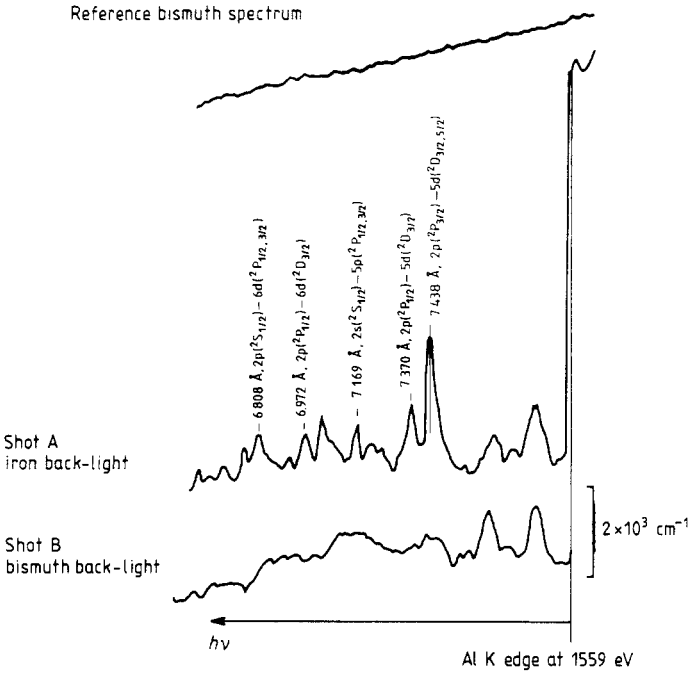


Figure 2. Time-integrated EXAFS spectra of 2 μm Al foil with different x-ray back-lighting sources.

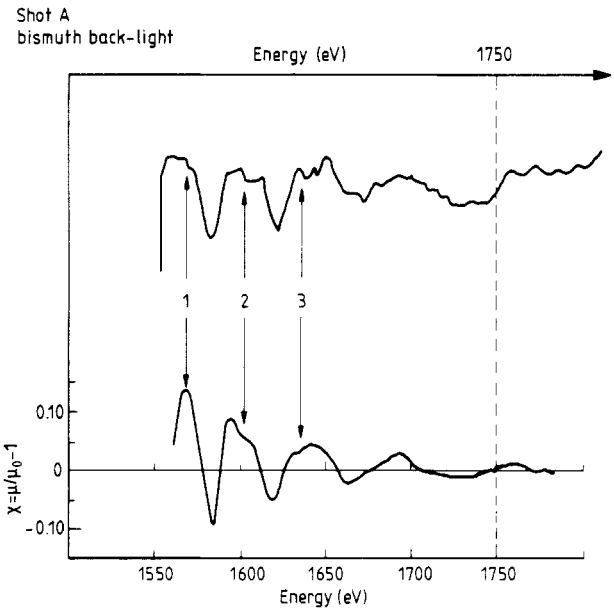


Figure 3. Comparison of the EXAFS spectrum of Al taken with a laser plasma source (top) and a synchrotron radiation source (bottom). This figure is reproduced from Fontaine *et al* (1979).

our laser-EXAFS data. The energy scale was calibrated using the positions of the Fe XXIV lines shown in figure 2. The laser-EXAFS spectrum has not been normalised, or even the background subtracted, but indicates the raw data taken directly from the microdensitometer scan. Several points are worth noting. Firstly the synchrotron radiation spectrum took approximately 90 min to record, compared with around 1 ns for the laser-EXAFS spectrum. Secondly, although the signal/noise is poorer for the laser-EXAFS spectrum, the agreement between the two spectra is very good. The four oscillation cycles seen in the Fontaine data are also clearly seen in the laser-EXAFS spectrum. They relate to scattering of the photoelectron by the 12 nearest neighbours in the FCC structure of Al. There is also excellent agreement between other features seen in the two spectra, notably the shoulders marked 2 and 3 in figure 3. These features are caused by scattering from shells of atoms more distant than the nearest neighbours. Thirdly, the spectral resolution ΔE in our experiment is 3–4 eV, and compares very favourably with the 4 eV quoted by Fontaine *et al* (1979). In our case the dominating factor governing the resolution was the source size ($\approx 200\text{ }\mu\text{m}$) as the contributions from both the detector element size (film grain size) and the rocking curve of the crystal are small in comparison. It would be an easy matter to generate a smaller source by focusing the laser pulse down still further, in which case correspondingly better spectral resolution would be achieved. Improved spectral resolution has been reported using a quartz crystal and a standard x-ray tube (Senemaud and Costa Lima 1976) but data were restricted to the near edge or XANES region.

If a similar comparison is made between the data from Fontaine *et al* (1979) and the laser-EXAFS data reported by Mallozzi *et al* (1979, 1980, 1981) and Epstein *et al* (1983),

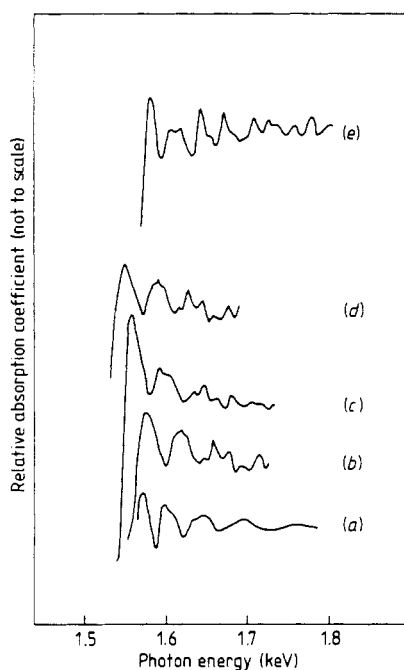


Figure 4. Comparison of previous published EXAFS spectra of aluminium taken with a laser plasma source (b)–(e), and a synchrotron radiation source (a).

the agreement is less convincing. This is shown in figure 4, where spectra taken from Mallozzi *et al* (1979, 1980, 1981) and Epstein *et al* (1983)—(b) to (e)—are compared with the synchrotron radiation spectrum of Fontaine *et al* (1979)—(a). Even allowing for obvious discrepancies in energy calibration, the fundamental period differs from spectrum to spectrum, the signal/noise is inferior to that for the present results (figure 2) and overall agreement with the results of Fontaine *et al* (1979) is only tenuous. It is not clear why this should be so but perhaps the use of iron as a target material complicates the normalisation of Al spectra.

3. Data reduction

To analyse the EXAFS, the spectrum was digitised using a Joyce–Loebl autodensitometer into a 750 point array. To convert the SB5 film density into an x-ray absorption coefficient (μ), the film curve for SB5 (Koppel 1982) and the published values for the mass absorption coefficient (μ/ρ) for aluminium were used (Veigele 1974).

The normalised EXAFS function, $\chi(E)$, is given by

$$\chi(E) = (\mu(E) - \mu_0(E)) / \mu_0(E)$$

where μ is the measured absorption coefficient and μ_0 is the absorption coefficient of isolated atoms, i.e. free from structural effects. $\chi(E)$ is therefore the fine-structure absorption per absorbing atom. μ_0 is obtained in the usual way from pre-edge ramp and by smoothing the post-edge absorption (Lee *et al* 1981). E is the energy of the excited photoelectron above the K-edge absorption threshold at 1.559 keV. The wavevector of the scattered photoelectron k is given by

$$E = E_0 + \hbar^2 k^2 / 2m$$

where m is the free electron mass and E_0 the photoelectron energy zero. E_0 does not coincide with absorption threshold but falls below this by ~ 10 eV. A local radial distribution of atoms can be obtained from the modulus of the complex Fourier transform of $\chi(k)$. This was used by Epstein *et al* (1983) but places shells of atoms at distances typically 10% to 20% shorter than their true values. (Fontaine *et al* (1979) quote 2.45 Å in place of the actual nearest-neighbour distance of 2.86 Å.) The reason for this misplacement is the phase change experienced by the photoelectron as it is scattered by the atomic potential firstly of the excited atom (δ) and then of the surrounding atoms (ψ). A more realistic local radial distribution is given by $|G(r)|$, where

$$G(r) = \frac{1}{2\pi} \int_{k_{\min}}^{k_{\max}} \frac{W(k)\chi(k) \exp[-i(2kr + 2\delta + \psi)] dk}{f(k, \pi)}$$

where $f(k, \pi)$ is the backscattering amplitude (Gurman and Pendry 1976). Values for the electron scattering factors f , δ and ψ for Al were calculated using the program MUFPT from the SRS Program Library at Daresbury Laboratory (Pantos and Firth 1983). $W(k)$ is a gaussian window function which for the present analysis was centred at approximately the middle of the spectral range. This is to help minimise the finite wavevector range defined by k_{\min} and k_{\max} which in this case was 4–8 Å⁻¹. Further details of this approach are given by Gurman and Pendry (1976).

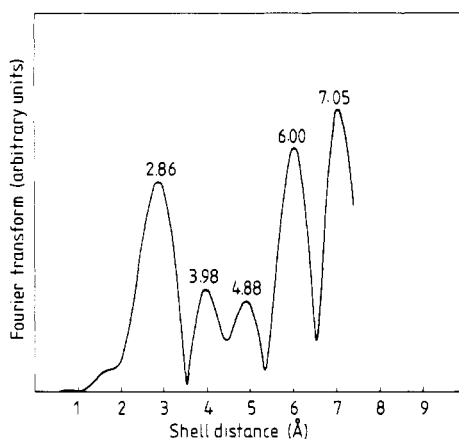


Figure 5. Fourier transform of the normalised EXAFS spectrum of aluminium. The shell positions are given in table 1 (where a is the nearest-neighbour distance).

4. Results

The result of the FT procedure can be seen in figure 5 in which the amplitude of the FT (arbitrary units) is plotted as a function of shell distance (\AA). A value of 16 eV was chosen for E_0 and the precise position of $W(k)$, 170 eV, was chosen to line the first peak up with the nearest-neighbour distance, which for FCC Al is 2.86 \AA (Brandes 1983). From table 1, one can compare the experimentally determined shell positions for the other shells with the crystallographic values. The second and third shells in the laser-EXAFS distribution are located to within 1.5% of the actual distances. The fourth and fifth shells are not resolved here but their mean position closely fits the fourth peak in $|G(r)|$. Likewise the fifth peak at 7.05 \AA lies close to the sixth shell (7.01 \AA) in the FCC structure. The agreement between the EXAFS radial distribution function and the crystallographic parameters is extremely good. In particular the resolution of the outer shells in Al is similar to that which can be obtained for Cu (Gurman and Pendry 1976). Other laser-EXAFS studies of Al have left even the nearest-neighbour distance ambiguous.

Table 1. The shell positions.

Shell	Radius (\AA)	
	Theory	Expt.
1	2.86(a)	2.86
2	4.04($2^{1/2}a$)	3.98
3	4.95($3^{1/2}a$)	4.88
4	5.72($2a$)	
5	6.40($5^{1/2}a$)	6.00
6	7.01($6^{1/2}a$)	7.05

5. Conclusion

In this paper we have demonstrated that EXAFS spectra in the soft x-ray range can be obtained using a laser plasma source and that these are equivalent in energy resolution to those obtained conventionally using synchrotron radiation. For a simple metal like Al reliable structural data can be obtained out to 6 or 7 Å. This marks an advance over previous laser-EXAFS measurements where there seems to be inconsistency between separate experiments. We believe the improvements we have made stem from the choice of a heavy-atom target material (Bi) which gives a spectrum free from line structure in the wavelength range of interest. As previous workers have pointed out (Epstein *et al* 1983) the laser plasma technique brings a colossal reduction in data collection times. The improvements in the laser EXAFS reported in this paper offer the prospect of reliable structural measurements of transient species on the sub-nanosecond timescale. Using the laser plasma as the source of heat, the dilated structure of exploding Al has been recorded. Details of this work will be published shortly (Eason *et al* 1984).

References

- Boiko V A, Faenov A Ya and Pikuz S A 1978 *J. Quant. Spectrosc. Radiat. Transfer* **19** 11
- Bradley D K, Kilkenny J D, Eason R W, Reason C J and Greaves G N 1984 unpublished
- Brandes E A (ed.) 1983 *Smithells Metals Reference Book* 6th ed (London: Butterworths) pp 6–13
- Eason R W, Bradley D K, Kilkenny J D and Greaves G N 1984 unpublished
- Eason R W and Toner W T 1983 *Annual Report to the Laser Facility Committee, Rutherford Appleton Laboratory* RL-83-043 ed. A F Gibson, pp 1–20
- Epstein H M, Schwerzel R E, Mallozzi P J and Campbell B E 1983 *J. Am. Chem. Soc.* **105** 1466
- Flank A M, Fontaine A, Jucha A, Lemonnier M and Williams C 1982 *J. Physique*. **43** L315
- Fontaine A, Lagarde P, Raoux D and Esteva J M 1979 *J. Phys. F: Met. Phys.* **9** 2143
- Gurman S J and Pendry J B 1976 *Solid State Commun.* **20** 287
- Kincaid B M and Eisenberger P M 1975 *Phys. Rev. Lett.* **34** 1361
- Koppel L N 1982 *Advanced Research and Applications Corp., Calif. Report No TR-112-08-02*
- Lee P A, Citrin P H, Eisenberger P and Kincaid B M 1981 *Rev. Mod. Phys.* **53** 769
- Lee P A and Pendry J B 1975 *Phys. Rev. B* **11** 2795
- Mallozzi P J, Schwerzel R E and Epstein H M 1980 *AIP Conf. Proc.* **64** 96
- Mallozzi P J, Schwerzel R E, Epstein H M and Campbell B E 1979 *Science* **206** 353
- 1981 *Phys. Rev. A* **23** 824
- Pantos E and Firth D 1983 *EXAFS and Near Edge Structure* ed. A Bianconi, L Incoccia and S Stipcich (Berlin: Springer) p 110
- Ross I N, White M S, Boon J E, Craddock D, Damerell A R, Day R, Gibson A F, Gottfeldt P, Nicholas D J and Reason C J 1981 *IEEE J. Quantum Electron.* **QE-17** 1653
- Senemaud C and Costa Lima M T 1976 *J. Phys. Chem. Solids* **37** 83
- Turner R E and Mead W C 1982 *Lawrence Livermore National Laboratory 1981 Laser Program Annual Report* pp 6–34
- Veigle W J 1974 *Handbook of Spectroscopy* vol 1, ed. J W Robinson (Cleveland, Ohio: Chemical Rubber) p 40